Customizable OpenGUS immunoassay: a homogeneous detection system using split β-glucuronidase and label-free antibody

Bo Zhu[1,‡], Yukihiko Yamasaki[2,‡], Takanobu Yasuda[1], Cheng Qian[3], Zhirou Qiu[3], Hiroshi Ueda[1,†], Tetsuya Kitaguchi[1,*]

[1] Laboratory for Chemistry and Life Science, Institute of Innovative Research, Tokyo Institute of Technology, Yokohama, Japan

[2] BioDynamics Laboratory Inc., Tokyo, Japan

[3] Graduate School of Life Science and Technology, Tokyo Institute of Technology, Yokohama, Japan

‡ Equal contributions

† Deceased

***Correspondence:**

Tetsuya Kitaguchi

kitaguc.t.aa@m.titech.ac.jp

Keywords: immunoassay, β-glucuronidase, antibody, Cry j 1, C-creative protein, lactoferrin, homogeneous

Abstract

We developed a customizable OpenGUS immunoassay for rapid and sensitive detection of analytes, eliminating the need for any antibody modifications. This assay employs a label-free whole antibody(ies), an antibody-binding domain derived from *Staphylococcal* protein A, and a split β-glucuronidase (GUS) mutant, allowing for the replacement of antibodies to establish an immunoassay for various targeted antigens. The working principle is that OpenGUS probe, the fusion protein of antibody-binding protein and split GUS mutant, converts the antibody-antigen interaction into GUS activation in a one-pot reaction. The split GUS mutant with decreased background activation was generated by screening several mutations at a diagonal interface residue H514. We optimized reaction buffer compositions, including organic solvent addition, salt concentrations, and surfactant concentrations, to enhance the signal/background ratio of the assay. In the optimal condition, we successfully customized OpenGUS fluorogenic immunoassays for Japanese cedar pollen allergen Cry j 1, human C-creative protein, and human lactoferrin with over 10–20-fold maximum fluorescence responses with picomolar to low nanomolar level detection limit within 15 min reaction time, by simply using commercially available IgGs. Moreover, in the absence of a fluorometer such as outdoors or at home, analytes can be detected using a simple smartphone or even the naked eye, with a pen-type UV-LED as the light source. We believe that the customizable OpenGUS immunoassay will pave new ways for the prompt development of rapid and sensitive homogeneous immunoassays for point-of-care diagnostics, high-throughput testing, and on-site environmental assessment applications.

Introduction

Immunoassays have been instrumental in advancing scientific research [1,2], clinical diagnostics [3,4], food safety control [5,6], and environmental monitoring [7] for several decades. These assays leverage the specific binding properties of antibodies to detect and quantify target analytes, which could range from small molecules to large proteins. From the very first radioimmunoassay (RIA) [8] to the classic enzyme-linked immunosorbent assay (ELISA) [9], the multiple binding and separation steps are included in these heterogeneous immunoassays. While they have demonstrated reliability and robustness, their intricate multi-step procedures can cause long operations and extra equipment requirements. An immunochromatography or lateral flow assay (LFA) utilizes a paper device to simplify the separation and washing steps in a heterogeneous immunoassay to achieve the analyte detection in a shorter period (5–30 min), but usually only provides qualitative or semi-quantitative results [10,11].

In contrast, homogeneous immunoassays are capturing increasing attention in both research and diagnostic fields [12,13]. The key advantage of these assays is the elimination of the separation or washing steps, rendering the process more streamlined and less time-consuming. This simplicity makes them particularly appealing for point-of-care testing and high-throughput scenarios [4,14]. The resonance energy transfer-based homogeneous immunoassays use two modified antibodies (or antigen for competitive assay) with combinations of chemiluminescent dye [15], fluorescent dye [16,17], fluorescent protein [18], and/or luciferase [18,19]. The analyte binding will trigger the distance change between the donor and receptor of the resonance energy transfer pair, thus changing the ratiometric signal. These resonance energy transfer-based assays did not adopt signal amplification mechanisms, which can lead to a moderate response in practical usage. Recently, a homogeneous immunoassay RAPPID used a robust split NanoLuc-modified antibodies to reach

over 5–30-fold ratiometric response against different analytes including protein biomarkers and virus antigen, and the bioluminescence signal can be detected by digital camera benefiting from the bright NanoLuc [14]. Previously, we reported several homogeneous immunoassays using fusion proteins of antibody fragments and split *E. coli* β-glucuronidase (GUS) for small molecule detection with enzyme-based signal amplification (OpenGUS antibody fragments) [20-22]. However, all the homogeneous immunoassays described above need antibody engineering or modification procedures (most also need purification steps), which made the customization of the assay and the screening of the optimal antibody difficult.

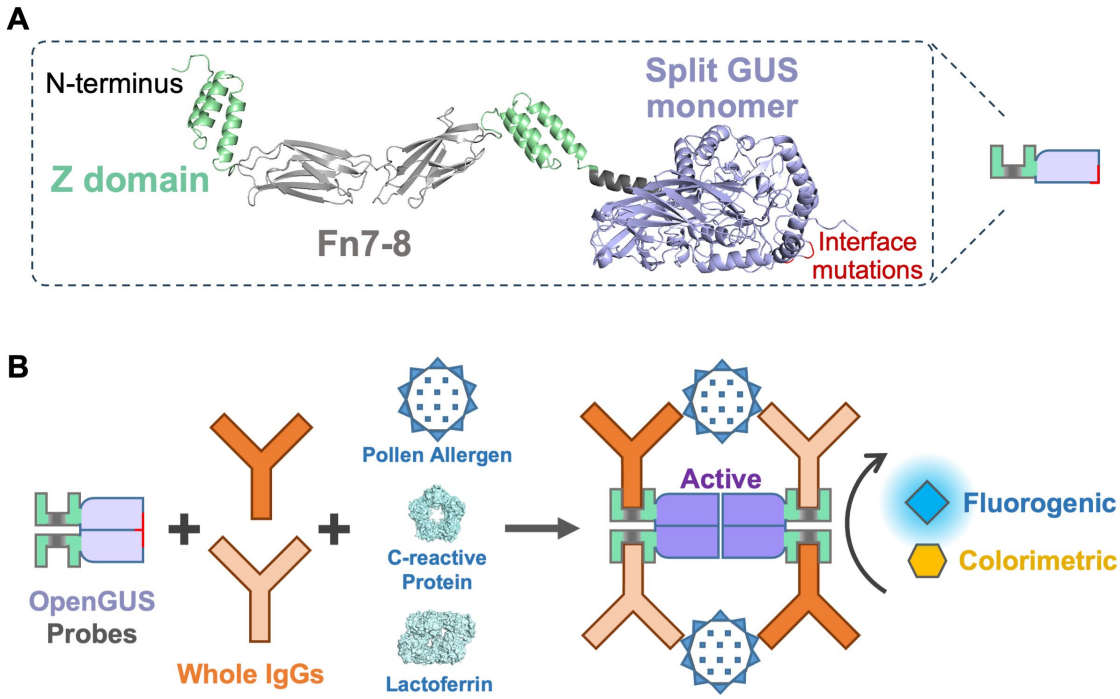

Fig. 1. Overview of OpenGUS immunoassay. (A) OpenGUS probe, a fusion protein of a split GUS mutant and two protein A-derived antibody-capturing Z domains (PZ) with fibronectin type III 7-8th domain (FN7-8) as a rigid spacer. (B) Scheme of OpenGUS homogeneous immunoassay by mixing OpenGUS probe, whole IgG antibody(ies), analyte, and substrate in one pot.

In this study, we developed a customizable OpenGUS immunoassay, for rapid and sensitive detection of protein analytes without the need for antibody engineering or modifications. In this immunoassay, an OpenGUS protein probe made of background-reduced split GUS and two protein

A-derived antibody-binding Z domains (PZ) (**Fig. 1A**), is used to convert the antibody-antigen binding signal into a GUS reconstruction and activation, which effectively amplifies the signal by producing fluorescent or colorimetric products in a short period. By simply mixing the antibodies against targets of interest, OpenGUS probe, analytes, and substrate in one pot (**Fig. 1B**), we successfully customized immunoassays for Japanese cedar pollen allergen Cry j 1, human C-creative protein, and human lactoferrin, with picomolar to low nanomolar limit of detections (LOD) and over 10–20-fold fluorescence responses within 15 min reaction time. Moreover, in the absence of a fluorometer such as outdoors or at home, analytes can be detected using a simple smartphone or even the naked eye, with a pen-type UV-LED as the light source. We believe that OpenGUS immunoassay will pave new ways for the prompt development of rapid and sensitive homogeneous immunoassays for point-of-care diagnostics, high-throughput testing, and on-site environmental assessment applications.

Results and Discussion

Preparation of split GUS and PZ fusion protein with different GUS H514 mutations

The wild-type GUS is a homotetramer enzyme reporter in colorimetric and fluorogenic assays, which can be engineered into split inactive homodimers by introducing interface mutants [22,23]. A thermostable split GUS mutant GUS_{IV5}-KW [21] was used in the bottom-up construction of the OpenGUS probe prototype (**Fig. 1A**). The B domain of *staphylococcal* protein A-derived antibody-binding protein, Z domain (PZ), has a specific binding affinity (10 nM) against the fragment crystallizable (Fc) region of IgG1 antibodies [24,25], and also showed binding ability against IgG2 and IgG4 [26]. Two PZ proteins were used in the OpenGUS probe to increase the binding avidity to the two binding sites on the Fc region of an IgG antibody. A rigid linker protein, 7th and 8th domains of fibronectin type III, with 7 nm N–C terminal distance [27] was inserted

into the two PZ proteins to increase the searching efficiency of secondary binding site recognition. To confirm the function of the designed probe prototype, the homogeneous detection for Japanese cedar pollen allergen Cry j 1 was performed by using two mouse anti-Cry j 1 monoclonal IgG1 antibodies recognizing different epitopes (**Fig. 2A**). The fluorescence signal difference between the reactions with and without analytes was not observed for this prototype. In the previous study, introducing proper mutation at a diagonal interface residue H514 of GUS_{TR3337} reduced the background signal of the split GUS_{TR3337} [22]. Therefore, we decided to investigate the effects of the H514 mutants of GUS_{IV5}-KW on the OpenGUS immunoassay.

A positive charge mutant H514K (**Fig. 2B**), three small side chain mutants (**Fig. 2C-E**), a conformational freedom reduced mutant H514P (**Fig. 3F**), and a negative charge mutant H514D (**Fig. 2G**) were prepared (**Fig. S1**) and tested in the OpenGUS assay for Cry j 1 detection. Except for the H514D mutant, all the other variants gave responses to the addition of Cry j 1 (**Fig. 2H-I**), which demonstrated the feasibility of the OpenGUS immunoassay design. The H514K, H514A, and H514S variants showed unreduced reaction rates and higher signal-background (S-B) after analyte-triggered reconstruction (**Fig. 2H**). Among the above three mutants, only the H514A variant showed stable or increased signal/background (S/B) during the signal development reaction (**Fig. 2I**). These results demonstrated again the importance of H514 mutations for modulation of the tetramerization functions of GUS. Therefore, we continued with the OpenGUS probe carrying GUS_{IV5}-KW-H514A mutant in the following development of the assay.

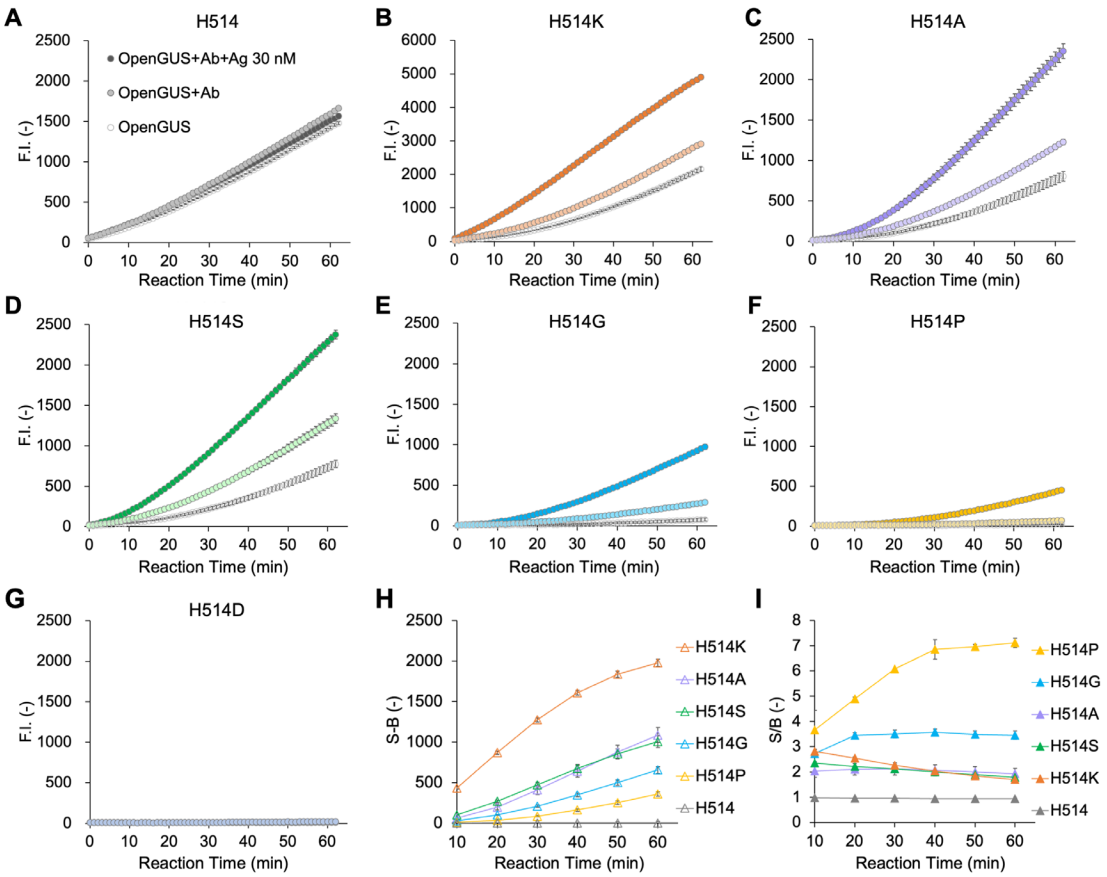

Fig. 2. Effect of the GUS_{IV5}-KW interface mutations on OpenGUS immunoassay for Cry j 1 allergen detection. (A)-(G) Assays with the OpenGUS probe carrying different GUS_{IV5}-KW H514 mutants. (H) Signal-background plot of assays with different GUS mutants. (I) Signal/background plot of assays with different GUS mutants. F.I., fluorescence intensity; Ab, antibody; Ag, antigen; Cry j 1 concentration: 30 nM; n = 3; Data were expressed as mean ± standard deviation.

Improving the signal/background ratio by including organic solvent in OpenGUS reaction

Some organic solvents in aqueous solution can stabilize the protein [28]. The split GUS has the exposed hydrophobic residues which could be stabilized by a small amount of organic solvent thus reducing the autonomous reconstruction background. Three well-used solvents for dissolving substrate in enzymatic reactions including dimethyl sulfoxide (DMSO), ethanol, and N,N-dimethylformamide (DMF) were tested for background reducing effect (**Fig. 3A-C**). The addition of 6% DMSO significantly reduced the background while not interfering with signal development

after the addition of the Cry j 1 (**Fig. 3D-E**), which resulted in an improved S/B ratio. This interesting phenomenon could be related to the reported protein stabilization function of DMSO at lower concentrations (<10–20%) through the preferential hydration effect [29]. But, to minimize the potential denaturation effect of the DMSO on antibody and analyte, the DMSO will be included in the substrate solution in the following experiment as the last reagent to be added into the OpenGUS immunoassay before the signal measurement.

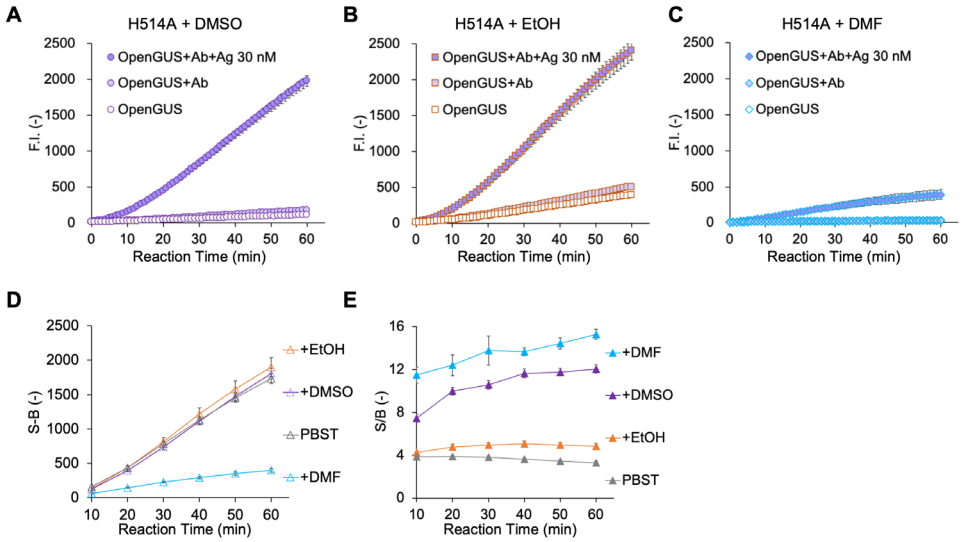

Fig. 3. Effect of the organic solvents in OpenGUS immunoassay for Cry j 1 allergen. (A) Assays in the presence of 6% (v/v) DMSO. (B) Assays in the presence of 6% (v/v) ethanol (EtOH). (C) Assays in the presence of 6% (v/v) DMF. (D) Signal-background plot of assays in the presence of different organic solvents. (I) Signal/background plot assays in the presence of different organic solvents. F.I., fluorescence intensity; Cry j 1 concentration: 30 nM; n = 3; Data were expressed as mean ± standard deviation.

Revisit the reaction buffer composition for OpenGUS immunoassay

Based on the successful S/B ratio improvement using DMSO, the concentrations of two components in the reaction buffer, NaCl and Tween 20, were also optimized. The physiological salt concentration is not always the best for protein stabilization and functionalization [30]. Therefore, no additional NaCl, 0.3×, 1×, and 3× physiological NaCl concentrations in reaction

buffers were investigated. Notably, the buffer without the addition of NaCl significantly increased both S-B and S/B for Cry j 1 detection (**Fig. 4A-B**). The concentrations of surfactant Tween 20 (0–1%, v/v) were also tested, and the decreases of both S-B and S/B were observed if the Tween 20 was not included in the reaction (**Fig. 4C-D**). And 0.1% or 0.5% Tween 20 was considered the optimal concentration for the OpenGUS immunoassay.

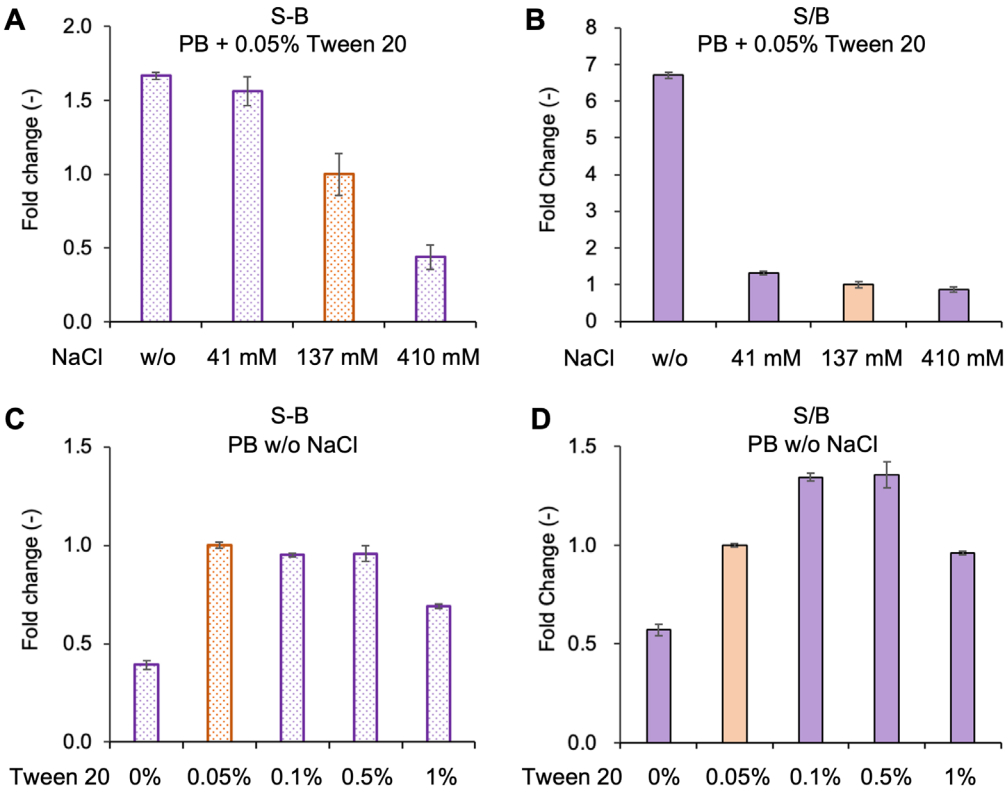

Fig. 4. Optimization of reaction buffer of OpenGUS immunoassay for Cry j 1 allergen detection. (A) Effect of NaCl concentration on the signal-background. (B) Effect of NaCl concentration on the signal/background. (C) Effect of Tween 20 concentration on the signal-background. (D) Effect of Tween 20 concentration on the signal/background. Bar graph in orange represents the sample used for normalization. PB: phosphate buffer without addition of NaCl; Cry j 1 concentration: 30 nM; Reaction time after adding fluorogenic substrate: 15 min; n = 3; Data were expressed as mean ± standard deviation.

Pre-incubation is not essential for OpenGUS immunoassay

In the above investigations, the OpenGUS probe, antibodies, and analytes were incubated at 4 °C for one hour before adding the substrate to maximize the antibody-antigen binding and split GUS

reconstruction. However, the long pre-incubation under temperature control is not ideal for point-of-care testing applications. Therefore, we compared different temperatures and lengths of pre-incubation to further simplify the assay using the OpenGUS probe. Firstly, the one-hour pre-incubation at 4 ℃ and room temperature (25 ℃) were compared, and the room temperature did not reduce the S-B and S/B for Cry j 1 detection (**Fig. 5A-B**). Next, the incubation was shortened to 30 min or eliminated, and even though the S-B was reduced slightly, the S/B did not become worse when no pre-incubation was performed (**Fig. 5C-D**). These results indicated that pre-incubation is not an essential step in OpenGUS immunoassay for sufficient analyte detection.

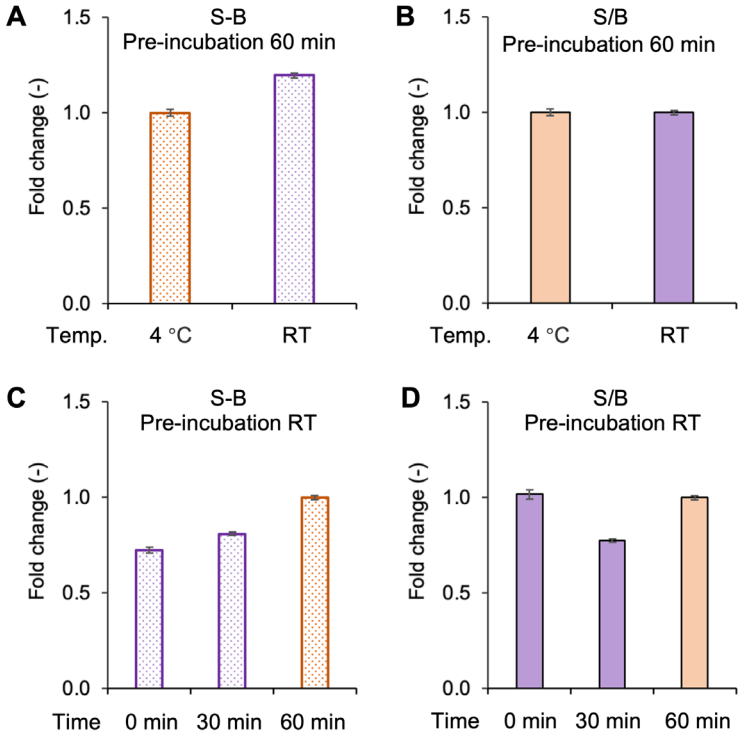

Fig. 5. Preincubation conditions optimization of OpenGUS immunoassay for Cry j 1 allergen detection. (A) Effect of preincubation temperature on the signal-background. (B) Effect of preincubation temperature on the signal/background. (C) Effect of preincubation length on the signal-background. (D) Effect of preincubation length on the signal/background. Bar graph in orange represents the sample used for normalization. Cry j 1 concentration: 30 nM; Reaction time after adding fluorogenic substrate: 15 min; n = 3; Data were expressed as mean ± standard deviation.

OpenGUS immunoassays for various protein analytes

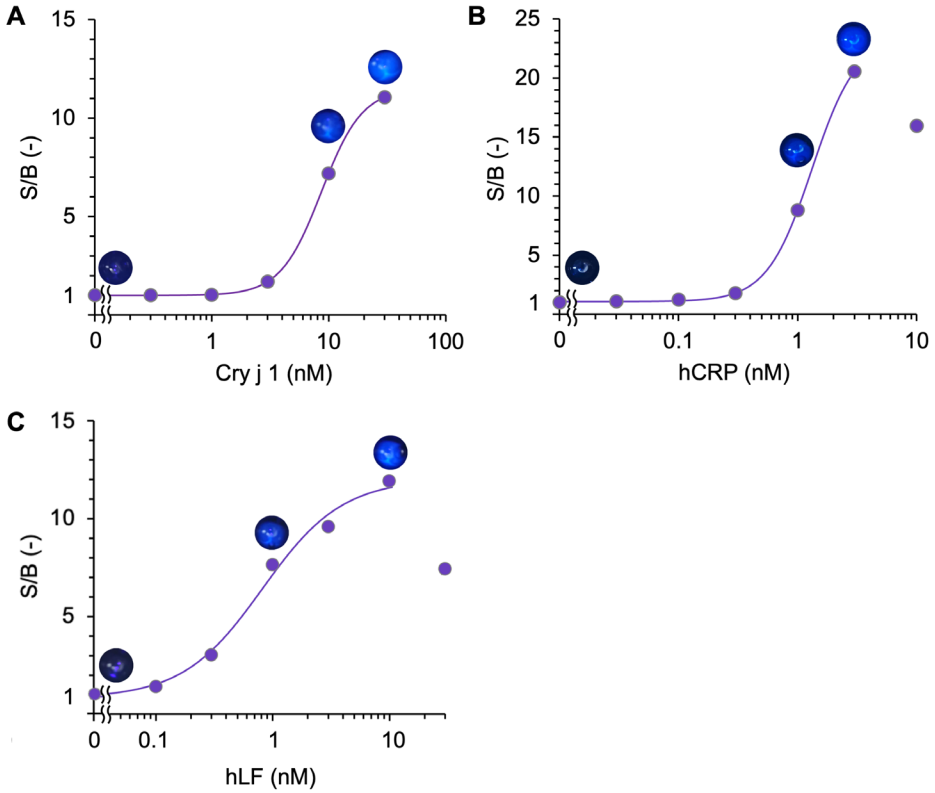

Fig. 6. OpenGUS immunoassays for detection of various protein analytes. (A) Dose-response curve for Cry j 1 detection with two antibodies. (B) Dose-response curve for human C-reactive protein (hCRP) detection with a single antibody, pentamer molar concentration. (C) Dose-response curve for human lactoferrin (hLF) detection with a single antibody, monomer molar concentration. Reaction time after adding fluorogenic substrate: 15 min; n = 3; Data were expressed as mean ± standard deviation. Pictures of the reaction wells taken using a smartphone were displayed above the data points in the dose-response curves.

The dose-response curve for pollen allergen Cry j 1 detection using OpenGUS immunoassay was measured under the optimized reaction condition without pre-incubation. After 15 min reaction, the LOD was determined as 1.4 nM, and the S/B response to 30 nM Cry j 1 was 12-fold (**Fig. 6A**). When using a pen-type UV-LED to irradiate the reaction wells, the blue color changes can be observed using a simple smartphone or even the naked eye, which makes the rapid analyte detection with OpenGUS immunoassay can be achieved in the absence of a fluorometer, e.g., harsh fieldwork environment, home, or basic laboratories in developing countries. The Cry j 1 detection

within a shorter reaction time is also possible, with a slight trade-off in the S/B and LOD. For example, in a 5-minute reaction, the LOD was 3.4 nM, and the fluorescence response to 30 nM Cry j 1 was 5-fold (**Fig. S2A**). The colorimetric readout using p-nitrophenyl β-D-glucuronide (PNPG) as substrate was also demonstrated for Cry j 1 detection. With a pre-incubation of 30 minutes, the assay detected the analyte with a LOD of 0.86 nM after a 30-minute reaction (**Fig. S3**). Since the condition optimization in this study was focused on the fluorogenic assay, further optimization for the colorimetric assay, including the pre-incubation and reaction time, could be done for the customized colorimetric assays if necessary.

Next, we customized the OpenGUS immunoassay to detect human C-reactive protein (hCRP, homopentamer, 114 kDa), which is an inflammation and cardiovascular disease biomarker [31]. The hCRP serum level in healthy adults is less than 0.3 mg/dL (260 nM), and can elevate to over 50 mg/dL (44 μM) during acute infections. Because hCRP is a protein oligomer, we were able to use single mouse monoclonal anti-hCRP IgG1 antibody instead of an antibody pair to trigger the split GUS activation (**Fig. 6B**). After a 15-minute reaction, the LOD was determined as 0.17 nM, and the response to 3 nM hCRP was 21-fold. The signal decrease was observed at a higher hCRP concentration than 3 nM (a hook effect), which could be due to each antibody being occupied by one or more antigens instead of the one antigen-two antibody complex, thus reducing the GUS reconstruction [32]. The hCRP detection within 5 minutes was also possible with a similar LOD of 0.13 nM. The fluorescence response to 3 nM hCRP was reduced to 8-fold (**Fig. S2B**) as expected.

We also customized OpenGUS immunoassay for the detection of human lactoferrin (hLF, mixed multimer, monomer 82 kDa). It has important immunological properties, such as antibacterial and antiviral functions (including SARS-CoV-2), and can act as biomarkers for various diseases [33]. The tear fluid hLF is a biomarker for ocular surface disease [34], and the saliva hLF could be used as a non-invasive biomarker of cerebral vulnerability in the general aging population [35], and

periodontal disease [36]. One report suggested that the hLF could start forming tetramer from around 10 pM and completely the oligomerization at around 1 nM concentration [37]. Therefore, same as the hCRP, one mouse monoclonal anti-hLF IgG1 antibody was used to customize the OpenGUS assay for hLF detection (**Fig. 6C**). The LOD was determined as 75 pM, and the response to 10 nM hLF was 12-fold after a 15 min reaction. In the 5-minute detection test, the LOD was determined as 130 pM, and the fluorescence response to 10 nM hLF was 5-fold (**Fig. S2C**). The working range of this assay is several orders of magnitude lower than the normal physiological concentration of hLF in tear fluid (~ 2 mg/mL, 24 μM monomer) and saliva (~ 0.8 mg/dL, 0.1 μM monomer) [38,39].

Conclusions

In this research, we developed a customizable OpenGUS immunoassay, employing label-free IgG antibodies together with a fusion protein probe of a low-background split GUS mutant and antibody Fc region-binding proteins. Reaction conditions including organic solvent addition, NaCl concentration, surfactant Tween 20 concentration, and the requirement of pre-incubation were optimized and discussed to improve the S/B ratio and the simplicity of the assay procedure. We demonstrated the detections of three protein analytes using commercially available IgG antibodies, achieving LOD ranging from picomolar to low nanomolar levels within a 15-minute reaction window. Notably, for oligomer analytes such as hCRP and hLF in this study, only a single antibody is needed to customize an OpenGUS immunoassay. Additionally, in scenarios lacking a fluorometer, like outdoor settings, homes, or less-equipped labs, the assay outcomes can be discerned using a smartphone or even the naked eye when using a pen-type UV-LED as the light source. Given its ease of customization, rapid and sensitive detection capabilities, and versatile readout options, we believe that OpenGUS immunoassay will pave new ways for the prompt

development of homogeneous immunoassays for point-of-care diagnostics, high-throughput testing, and on-site environmental assessment applications.

Materials and Methods

Materials

E. coli SHuffle® T7 Express lysY was purchased from New England Biolabs, USA. B-PER™ Bacterial Protein Extraction Reagent was purchased from Thermo Fisher Scientific, USA. TALON® Metal Affinity Resin was purchased from Takara Bio, Japan. Mouse anti-Cry j 1 monoclonal antibodies (clones 053 and 013) and Cry j 1 protein (catalog no. HBL-C-1) were obtained from BioDynamics Laboratory, Japan. Mouse anti-human C-creative protein monoclonal antibody (clone 160.10G10) and hCRP (catalog no. PHP277) were purchased from Bio-Rad Laboratories, Japan. Mouse anti-human lactoferrin monoclonal antibody (clone 1A1) was purchased from HyTest, Finland. Lactoferrin from human milk (catalog no. 7550-2) was purchased from BioVision, USA. Colorimetric substrate p-nitrophenyl β-D-glucuronide (PNPG, catalog no. N0618) was purchased from Tokyo Chemical Industry, Japan. Other chemicals were purchased from FUJIFILM Wako Pure Chemicals, Japan unless otherwise indicated.

Expression and purification of OpenGUS protein probe

The synthesized whole OpenGUS probe sequences was cloned into pETIA vector (BioDynamics Laboratory) between ATG start codon and TAA stop codon as expression plasmids. The expression plasmid was transformed into *E. coli* SHuffle® T7 Express lysY competent cells. Cells were grown in LB medium (Difco LB broth, Lennox, BD) containing 100 μg/mL ampicillin at 30 °C with shaking at the speed of 150 rpm to an OD_{600}~0.4–0.5, then the expression was induced with 0.5 mM isopropyl β-D-thiogalactopyranoside (IPTG) for 16 h at 16 °C. The cells were harvested by centrifugation at 4 °C. The pellet was lysed with B-PER™ Bacterial Protein

Extraction Reagent. The lysate was recovered using centrifugation at 10,000 × *g*, for 25 min at 4 °C, and the OpenGUS probe in the supernatant was purified with TALON® Metal Affinity Resin according to the manual after resin equilibration with purification buffer (50 mM sodium phosphate, 300 mM NaCl, pH 8.2). Proteins bound to the resin were eluted using elution buffer (purification buffer with 500 mM imidazole), and were kept on ice for 1 h. Glycerol was added to the eluted OpenGUS probe, to a final concentration of 25%, and the protein solution was stored at −80 °C. The purified proteins were analyzed using SDS-PAGE, and the concentration was determined by the band intensity after Coomassie brilliant blue staining using bovine serum albumin as standard on the same gel.

OpenGUS homogeneous immunoassay

A phosphate buffer (8.1 mM Na_2HPO_4, 1.47 mM KH_2PO_4, pH was adjusted to 7.4) is the base of all the reaction buffers used in this study. The 0.5% (v/v) Tween 20 was included in the optimized reaction buffer. The fluorogenic substrate 4-methylumbelliferyl β-D-glucuronide (4-MUG) or colorimetric substrate PNPG was dissolved in the optimized reaction buffer containing 12% (v/v) DMSO at the concentration of 0.6 mg/mL as a substrate solution. The OpenGUS probe (final conc. 7.5 nM), IgG antibody (final conc. 7.5 nM for each in an antibody pair or 15 nM for single antibody), analyte, and substrate solution (final conc. 0.3 mg/mL) were mixed in above order before the fluorescence intensity or absorbance measurement.

The fluorescence intensity was measured in a 96-well black microplate (catalog no. 675076, Greiner Bio-One, Austria) using a microplate reader CLARIOstar (BMG Labtech, Germany) at 25 °C with excitation and emission wavelengths of 360/20 nm and 450/30 nm (center/bandwidth), respectively. The pictures of the reaction wells were taken by a smartphone (G8441, SONY, Japan) with fixed ISO (200), shutter speed (1/16 s), and aperture (f/2.0), using a pen-type UV-LED (PW-

UV141P-01, KONTEC, Japan) as an excitation light source (LED unit: peak wavelength 375 nm, spectrum half-width 9 nm, radiant flux 1160 mW, part no. NVSU119C, NICHIA, Japan). In the colorimetric assays, the absorbance at 405 and 660 nm was measured in a 96-well clear microplate (catalog no. 3590, Corning, USA) using a microplate reader SH-1000 (Corona Electric, Japan).

Dose-response curve fitting

Dose-response curves were fitted to a four-parameter logistic equation (1) using SciDAVis software (version 2.4.0). The limit of detection was calculated as the concentration corresponding to the mean blank value plus three times its standard deviation.

$$y = d + \frac{a-d}{1+\left(\frac{x}{c}\right)^{b}} \qquad (1)$$

Author Contributions

T.K. and H.U. conceived the study. B.Z. and Y.Y. designed and performed the experiments. T.Y., C.Q., and Z.Q. supported performing the experiments. B.Z. wrote the original manuscript. H.U. and T.K. provided the resources and supervised the study. All authors discussed the results and edited the manuscript.

Conflicts of Interest

B.Z., T.Y., H.U., and T.K. received honoraria from HikariQ Health, Inc. for another unrelated project.

Acknowledgments

We thank Toru Hisabori from the Tokyo Institute of Technology for critical discussion and advice on this work. This work was supported in part by JSPS KAKENHI Grant Numbers JP22H05176 (to T.K.) and JP21K14468 (to B.Z.) from the Japan Society for the Promotion of

Science, a Research Grant from the Nakatani Foundation (to H.U. and T.K.), and the Mishima Kaiun Memorial Foundation (to T.K.).

References

[1] Boguszewska, K., Szewczuk, M., Urbaniak, S. and Karwowski, B.T. (2019). Review: immunoassays in DNA damage and instability detection. Cell Mol Life Sci 76, 4689-4704.

[2] Dai, Y.C., Sato, Y., Zhu, B., Kitaguchi, T., Kimura, H., Ghadessy, F.J. and Ueda, H. (2022). Intra Q-body: an antibody-based fluorogenic probe for intracellular proteins that allows live cell imaging and sorting. Chemical Science 13, 9739-9748.

[3] Voller, A., Bidwell, D.E. and Bartlett, A. (1976). Enzyme immunoassays in diagnostic medicine. Theory and practice. Bull World Health Organ 53, 55-65.

[4] Zhu, B. et al. (2022). Rapid and sensitive SARS-CoV-2 detection using a homogeneous fluorescent immunosensor Quenchbody with crowding agents. Analyst 147, 4971-4979.

[5] Samarajeewa, U., Wei, C.I., Huang, T.S. and Marshall, M.R. (1991). Application of immunoassay in the food industry. Crit Rev Food Sci Nutr 29, 403-434.

[6] Su, J. et al. (2022). The Patrol Yeast: A new biosensor armed with antibody-receptor chimera detecting a range of toxic substances associated with food poisoning. Biosens Bioelectron 219, 114793.

[7] Ahn, K.C., Kim, H.J., McCoy, M.R., Gee, S.J. and Hammock, B.D. (2011). Immunoassays and biosensors for monitoring environmental and human exposure to pyrethroid insecticides. J Agric Food Chem 59, 2792-2802.

[8] Berson, S.A., Yalow, R.S., Bauman, A., Rothschild, M.A. and Newerly, K. (1956). Insulin-I131 metabolism in human subjects: demonstration of insulin binding globulin in the circulation of insulin treated subjects. J Clin Invest 35, 170-190.

[9] Engvall, E. and Perlmann, P. (1972). Enzyme-linked immunosorbent assay, Elisa. 3. Quantitation of specific antibodies by enzyme-labeled anti-immunoglobulin in antigen-coated tubes. J Immunol 109, 129-135.

[10] Koczula, K.M. and Gallotta, A. (2016). Lateral flow assays. Essays Biochem 60, 111-120.

[11] Banerjee, R. and Jaiswal, A. (2018). Recent advances in nanoparticle-based lateral flow immunoassay as a point-of-care diagnostic tool for infectious agents and diseases. Analyst 143, 1970-1996.

[12] Takkinen, K. and Zvirbliene, A. (2019). Recent advances in homogenous immunoassays based on resonance energy transfer. Curr Opin Biotechnol 55, 16-22.

[13] Rani, A.Q., Zhu, B., Ueda, H. and Kitaguchi, T. (2023). Recent progress in homogeneous immunosensors based on fluorescence or bioluminescence using antibody engineering. Analyst 148, 1422-1429.

[14] Ni, Y. et al. (2021). A plug-and-play platform of ratiometric bioluminescent sensors for homogeneous immunoassays. Nat Commun 12, 4586.

[15] Akhavan-Tafti, H. et al. (2013). A homogeneous chemiluminescent immunoassay method. J Am Chem Soc 135, 4191-4194.

[16] Ullman, E.F., Schwarzberg, M. and Rubenstein, K.E. (1976). Fluorescent excitation transfer immunoassay. A general method for determination of antigens. J Biol Chem 251, 4172-4178.

[17] Ueda, H., Kubota, K., Wang, Y., Tsumoto, K., Mahoney, W., Kumagai, I. and Nagamune, T. (1999). Homogeneous noncompetitive immunoassay based on the energy transfer between fluorolabeled antibody variable domains (open sandwich fluoroimmunoassay). Biotechniques 27, 738-742.

299 [18] Arai, R., Nakagawa, H., Tsumoto, K., Mahoney, W., Kumagai, I., Ueda, H. and Nagamune,
300 T. (2001). Demonstration of a homogeneous noncompetitive immunoassay based on
301 bioluminescence resonance energy transfer. Anal Biochem 289, 77-81.
302 [19] Yu, X., Wen, K., Wang, Z., Zhang, X., Li, C., Zhang, S. and Shen, J. (2016). General
303 Bioluminescence Resonance Energy Transfer Homogeneous Immunoassay for Small Molecules
304 Based on Quantum Dots. Anal Chem 88, 3512-3520.
305 [20] Su, J., Dong, J.H., Kitaguchi, T., Ohmuro-Matsuyama, Y. and Ueda, H. (2018).
306 Noncompetitive homogeneous immunodetection of small molecules based on beta-glucuronidase
307 complementation (vol 143, pg 2096, 2018). Analyst 143, 3499-3499.
308 [21] Su, J.L., Beh, C., Ohmuro-Matsuyama, Y., Kitaguchi, T., Hoon, S. and Ueda, H. (2019).
309 Creation of stable and strictly regulated enzyme switch for signal-on immunodetection of various
310 small antigens. Journal of Bioscience and Bioengineering 128, 677-682.
311 [22] Zhu, B., Qian, C., Tang, H.X., Kitaguchi, T. and Ueda, H. (2023). Creating a Thermostable
312 beta-Glucuronidase Switch for Homogeneous Immunoassay by Disruption of Conserved Salt
313 Bridges at Diagonal Interfaces. Biochemistry 62, 309-317.
314 [23] Geddie, M.L. and Matsumura, I. (2007). Antibody-induced oligomerization and activation
315 of an engineered reporter enzyme. J Mol Biol 369, 1052-1059.
316 [24] Jansson, B., Uhlen, M. and Nygren, P.A. (1998). All individual domains of staphylococcal
317 protein A show Fab binding. Fems Immunology and Medical Microbiology 20, 69-78.
318 [25] Braisted, A.C. and Wells, J.A. (1996). Minimizing a binding domain from protein A. Proc
319 Natl Acad Sci U S A 93, 5688-5692.
320 [26] Scheffel, J., Kanje, S., Borin, J. and Hober, S. (2019). Optimization of a calcium-dependent
321 Protein A-derived domain for mild antibody purification. MAbs 11, 1492-1501.

[27] Ohmuro-Matsuyama, Y., Chung, C.I. and Ueda, H. (2013). Demonstration of protein-fragment complementation assay using purified firefly luciferase fragments. BMC Biotechnol 13, 31.

[28] Asakura, T., Adachi, K. and Schwartz, E. (1978). Stabilizing Effect of Various Organic-Solvents on Protein. Journal of Biological Chemistry 253, 6423-6425.

[29] Arakawa, T., Kita, Y. and Timasheff, S.N. (2007). Protein precipitation and denaturation by dimethyl sulfoxide. Biophys Chem 131, 62-70.

[30] Lindman, S., Xue, W.F., Szczepankiewicz, O., Bauer, M.C., Nilsson, H. and Linse, S. (2006). Salting the charged surface: pH and salt dependence of protein G B1 stability. Biophys J 90, 2911-2921.

[31] Pepys, M.B. and Hirschfield, G.M. (2003). C-reactive protein: a critical update. J Clin Invest 111, 1805-1812.

[32] Jacobs, J.F., van der Molen, R.G., Bossuyt, X. and Damoiseaux, J. (2015). Antigen excess in modern immunoassays: to anticipate on the unexpected. Autoimmun Rev 14, 160-167.

[33] Kell, D.B., Heyden, E.L. and Pretorius, E. (2020). The Biology of Lactoferrin, an Iron-Binding Protein That Can Help Defend Against Viruses and Bacteria. Front Immunol 11, 1221.

[34] Ponzini, E., Scotti, L., Grandori, R., Tavazzi, S. and Zambon, A. (2020). Lactoferrin Concentration in Human Tears and Ocular Diseases: A Meta-Analysis. Invest Ophthalmol Vis Sci 61, 9.

[35] Reseco, L., Atienza, M., Fernandez-Alvarez, M., Carro, E. and Cantero, J.L. (2021). Salivary lactoferrin is associated with cortical amyloid-beta load, cortical integrity, and memory in aging. Alzheimers Research & Therapy 13, 150.

344 [36] Koshi, R., Kotani, K., Ohtsu, M., Yoshinuma, N. and Sugano, N. (2018). Application of
345 Lactoferrin and alpha1-Antitrypsin in Gingival Retention Fluid to Diagnosis of Periodontal
346 Disease. Dis Markers 2018, 4308291.
347 [37] Bagby, G.C., Jr. and Bennett, R.M. (1982). Feedback regulation of granulopoiesis:
348 polymerization of lactoferrin abrogates its ability to inhibit CSA production. Blood 60, 108-112.
349 [38] Levay, P.F. and Viljoen, M. (1995). Lactoferrin: a general review. Haematologica 80, 252-
350 267.
351 [39] Rosa, L., Cutone, A., Lepanto, M.S., Paesano, R. and Valenti, P. (2017). Lactoferrin: A
352 Natural Glycoprotein Involved in Iron and Inflammatory Homeostasis. Int J Mol Sci 18, 1985.